ASSESSMENT OF CHEMICAL MECHANISM AND CHEMICAL REACTION SENSITIVITY ANALYSIS FOR CH_4/H_2 FLAME UNDER MILD COMBUSTION ENVIRONMENT

by

Zhao YANG, Xiangsheng LI *, Zhenlin WANG, and Zhuangqi WANG
Institute of Turbomachinery, Xi'an Jiaotong University, Xi'an, China

Original scientific paper
https://doi.org/10.2298/TSCI180811347Y

To analyze the performance of different chemical mechanisms on the prediction under moderate and intense low-oxygen dilution combustion environment, six different kinds of mechanisms were tested by solving the Reynolds averaged Navier-Stokes equations in a 2-D domain with the eddy dissipation concept model by FLUENT software. Temperature and the species concentration of OH, CO, and H_2O were compared with the experiment data. The experiment results showed some similarities for each chemical mechanism as well as discrepancies. The comparison of CH_4 oxidation route between the GRI2.11 and GRI3.0 mechanisms was made by Chemkin code. Reaction 95 and 147 were responsible for low temperature region for GRI2.11 mechanism at downstream area.

Key words: *moderate and intense low-oxygen dilution combustion, chemical mechanism, combustion simulation, reaction pathway analysis*

Introduction

Moderate and intense low-oxygen dilution (MILD) combustion is one of the most attractive novel combustion technologies nowadays. It provides high efficiency as well as lower emissions compared with traditional combustion mode. The MILD combustion occurs when the fuel is preheated above their self-ignition temperature and when enough inert combustion products are entrained to dilute the flame [1]. Different from conventional combustion, MILD combustion is usually constrained at a low oxygen environment (5-10% in mass fraction). The combustion air needs to be preheated by a regenerator to about 1300-1600 K. The development of numerical simulation on MILD combustion is of great importance in industrial use.

The MILD combustion technology is widely used in some industries, the relevant research carried out by Dally *et al.* [2] was a jet in hot co-flow (JHC) burner developed to simulate the MILD combustion. In their research, detailed measurements of temperature and concentration of major and minor species (including CO and OH) were published. Oldenhof *et al.* [3] provided very valuable experiment dataset by using both flame luminescence and planer laser induced fluorescence (OH-PLIF) method, which consists of velocity measurement and temperature of several natural gas flames in the delft jet in hot co-flow (DJHC) burner.

The CFD provides great benefit to the development of MILD combustion technology. One of the key characteristic in modeling MILD combustion is that the slower reaction rates

* Corresponding author, e-mail: lixs@mail.xjtu.edu.cn

caused by the strong coupling of turbulence and chemistry, which is characterized by similar timescale. So, it is of great importance to analyze the behavior of different chemical mechanism in simulating MILD combustion. Wang *et al.* [4] studied the six global CH_4/H_2 mechanisms for MILD combustion. They found that the Westbrook-Dyer mechanism (WD4), which consists of the oxidation of CO and H_2, showed the best simulation result. Amir *et al.* [5] used DRM22 mechanism and GRI2.11 mechanism to represent the chemical reactions of H_2/CH_4 jet flame. Results of calculation and experiment were compared and there was a good agreement between them. Parente *et al.* [6] used the DRM mechanism in the experiment, and he found that there were agreements between the DRM19 and GRI3.0 Mechanisms. On the other hand, compared with the DRM19 mechanism, the DRM22 mechanism performed better in predicting the ignition delay and the laminar flame speed at the atmospheric condition. The DRM22 mechanism has been proven to be used in the low and moderate oxygen diluted combustion environment in previous research.

It is a general opinion that MILD condition interaction should be treated with finite rate approaches. Coelho and Peters [7] used the flamelet model to study turbulence-chemistry interaction in the MILD regime. Although there were good agreements between numerical and experimental measurements qualitatively, the emission productions and species residence time showed some deviation. Christo and Dally [8] evaluated the turbulent and combustion model for the MILD combustion by comparing the simulation result and experiment data in a jet burner with hot co-flow. He found that the eddy dissipation concept (EDC) model adopts a global and detailed mechanism is the best. Kim *et al.* [9] used the conditional moment closure method coupling a laminar flamelet model with the GRI2.11 mechanism, their experiment showed some good agreements on upstream at $z = 30$ mm. However, at $z = 60$ mm and $z = 120$ mm, where the interaction between fuel and air became significant, the critical micelle concentration (CMC) method became inadequate to model the flow field. Ihme and See [10] employed a flametlet progress variable model with a large eddy simulation approach to model 9% O_2 case. However, the high computational cost needed simplified oxidation kinetics.

The well-stirred reactor is also applied in investigating the MILD combustion. The fine structures in EDC model are assumed as isobaric, adiabatic and perfectly stirred reactors with finite reaction time scale compared with turbulent time scale. From this point of view, it is easy to find some similarities between characteristics of the EDC model and WSR model. Wang *et al.* [11] used detailed kinetic mechanism to characterize the combustion of $CH_4/O_2/N_2$ mixture in a WSR, the product composition and elementary chemical pathways of methane oxidation were examined. Weber *et al.* [12] have verified that the possibility of WSR research could be a useful tool to catch a glimpse of methane mixture oxidation under MILD combustion environment.

Although lots of researches have been carried on the CFD simulation for MILD combustion, the mechanism on MILD combustion has seldom been discussed systematically. The present paper studied the six different kinds of mechanisms for the CH_4/H_2 combustion. The performances for each mechanism on the MILD combustion were analyzed. The mechanism included the WD3 global mechanism, 41-step skeletal mechanism, KEE-58 and DRM22 reduced mechanism as well as the detailed GRI2.11 and GRI3.0 mechanism. Although some of these mechanisms have been justified for classical premixed or diffusion combustion conditions, their performance on MILD conditions needs further theoretical investigations.

The paper will firstly introduce all the six different kinds of mechanisms in the text. Simulation on the JHC burner would be carried to study the behavior of different mechanism on the MILD combustion environment. Both the experimental and simulation temperature and species concentration were systematically compared. After that, the WSR model was employed

to analyze the dominant elementary reactions and to interpret the different flame luminance phenomenon at the experiment.

Numerical method

Experiment geometry and boundary condition

The hot co-flow burner experimental apparatus was shown in fig. 1 [13]. It consists of a fuel jet nozzle, which has an inner diameter of 4.25 mm, located at the center of a perforated disc in an annulus, with an inner diameter of 82 mm. It provides a uniform composition of hot co-flow to the reaction region. The whole combustor was set inside a wind tunnel which introduced air with the room temperature at the same velocity of the co-flow. In tab. 1, the operating conditions of the experiment were shown. The fuel jet inlet Reynolds number was around 10000.

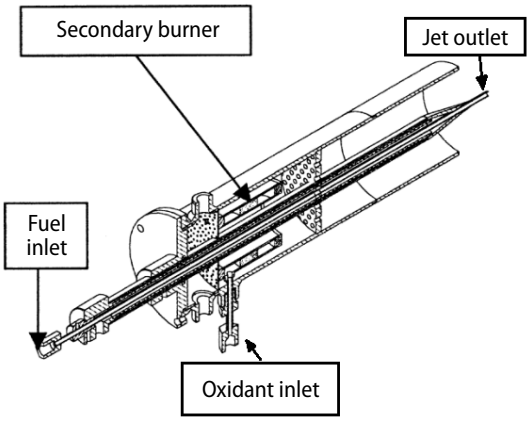

Figure 1. Scheme of the JHC burner

Table 1. Operating conditions for the experiment

	Fuel jet	Oxidation co-flow	Tunnel air
Flow rate	$3.12 \cdot 10^{-4}$ kg/s	3.2 m/s	3.2 m/s
Temperature	305 K	1300 K	294 K
Mass fraction	88.9% CH_4 11.1% H_2	6% O_2 6.5% H_2O 5.5% CO_2 82% N_2	23.2% O_2 77.8 N_2

Figure 2 shows the numerical geometry and boundary conditions for the numerical experiment. A 2-D-axisymetric computational domain with 30000 structuring grid were applied. In order to further check whether the number of grid was dependent of the result, a finer mesh of 80000 were tested. The results of velocity, temperature and species concentration showed no obvious difference, which proved that the simpler grid is capable of modeling the JHC flame. The calculation was applied on FLUENT 17.0 software. To solve the RANS equations, the realizable k-ε model with $C\varepsilon_1$ modified from 1.44 to 1.6 was considered to compensate plane jet error [8]. Time and spatial distribution used the second order upwind scheme. Detailed and skeletal mechanisms were coupled with EDC model which is based on finite reaction rate assumption. Simple algorithm was used to solve the pressure and velocity coupling. Thermal radiation was taken into account using the discrete ordinates method and the radiative properties of the participating medium were modeled by the weighted-sum-of-grey gases model. The spatial variation of the total emissivity is considered as a function of the main species and temperature. We have added this part in our paper. Residual level was set as $1.0 \cdot 10^{-6}$. The average mass flow rate of CO was regard as one of convergence principles.

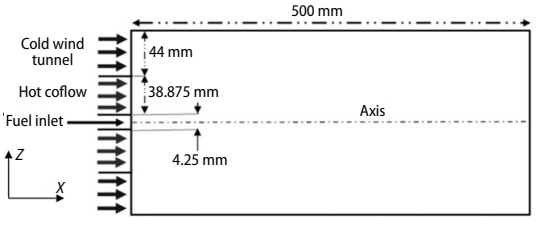

Figure 2. Numerical model geometry and boundary conditions

Chemical mechanism and turbulent model

The six different kinds of mechanisms discussed in the present paper are as follows.

- A 3-step global chemical mechanism concluded by Westbrook and Dryer [14]. The mechanism included two global reaction steps as well as quasi-global mechanisms. Its reaction rate parameters were varied in order to provide best flame speed under different mixture ratio.
- A 16-specie and 41-step skeletal chemical mechanism introduced by Yang and Pope [15], mainly used for CH_4/air combustion.
- A 17-specie and 58-step skeletal chemical mechanism named as KEE-58 mechanism [16]. It is commonly used in premixed syngas flame.
- A shortened full chemical mechanism of GRI1.2, DRM22 mechanism which consists of 22 species and 104 elementary reactions which is concluded by Kazakov and Frenklach [5]. Compared with the above skeletal chemical mechanisms, the DRM22 mechanism contains C_2 oxidation route.
- The GRI2.11 mechanism is a list of CH_4-air elementary chemical reactions and associated rate constant expressions. It consists of 49 species and 279 elementary reactions.
- The GRI3.0 mechanism has been updated and improved by the GRI2.11 versions. The conditions for GRI3.0 was optimized, limited primarily by availability of reliable optimization targets, are roughly 1000 to 2500 K, 0.013 atm to 10 atm, and equivalence ratio from 0.1 to 5 for premixed systems. It has been tested on simulation in dilution of air, methane-air and oxy diffusion flames.

In the research of Gran and Magnussen [17], finite reaction rate kinetics was introduced into the EDC model. In their research, the flow region was separate as *fine structure* and *surrounding fluid*. All the reaction occurs at this adiabatic and isobaric fine structure. In fine structure, there are only mass and energy transfer with neighboring fluid. The scale of the fine structure is defined as ζ and the residual time is defined as τ. The net reaction rate can be defined:

$$\tilde{\dot{\omega}}_i = \frac{\overline{\rho}\overline{\xi^2}\lambda}{\tau}\left(Y_i^* - Y_i^o\right) \tag{1}$$

where Y_i^* and Y_i^0 represent the mass fraction of spices i in reacting and non-reacting zones. The average residual time τ is inverse proportion with the reaction rate ω_i.

The length scale and the time scale for fine structure can be described:

$$\gamma^* = \left(\frac{3C_{D2}}{4C_{D1}}\right)^{\frac{3}{4}}\left(\frac{\nu\varepsilon}{k^2}\right)^{\frac{3}{4}} = C_\gamma\left(\frac{\nu\varepsilon}{k^2}\right)^{\frac{3}{4}} \tag{2}$$

$$\tau^* = \left(\frac{C_{D2}}{3}\right)^{\frac{1}{2}}\left(\frac{\nu}{\varepsilon}\right)^{\frac{1}{2}} = C_t\left(\frac{\nu}{\varepsilon}\right)^{\frac{1}{2}} \tag{3}$$

where C_{D1} and C_{D2} are set as 0.134 and 0.5, therefore $C_r = 2.1637$ and $C_t = 0.4083$. These two parameters have some physical meanings. In Aminian *et al.* [18], the two parameters have been systematically study. A reference value of $C_t = 1.5$ and $C_r = 1$ were introduced to MILD combustion environment. The effect of low Reynold number co-flow region reaction rate will be compensated. The modified parameter will be used in our research.

Results and discussion

Figure 3 shows the temperature distributions for the six different mechanisms. All the simulating results consist of three reaction regions. They are the MILD region, the neck region and the downstream region, respectively. The MILD region locates at $x < 100$ mm. In this region, the flow dynamics are not strongly influenced by the surrounding air. The entrainment of co-flow can lead to local extinction at the mixing zone by effect of high mixing intensity. At $100 < x < 200$ mm, where fuel and dilution air are intensely mixed, a strong transition zone emerges at this neck zone. Flame re-ignition may occur further downstream of the extinction zone where turbulent mixing rates are less intense when $x > 200$ mm. When $x > 200$ mm, the downstream area has three different kinds of results. The WD3, 41-step and KEE-58 mechanism have a peak temperature of 2000 K, DRM22, and GRI3.0 have a peak temperature of 1800 K. However, the flame has a low temperature field at the downstream area. This phenomenon can be explained by the flame liftoff effect. In Kim's research [19], the results obtained from GRI2.11 was different from other mechanism. The heat release rate was dependent on the liftoff and blowout characteristics of the flames.

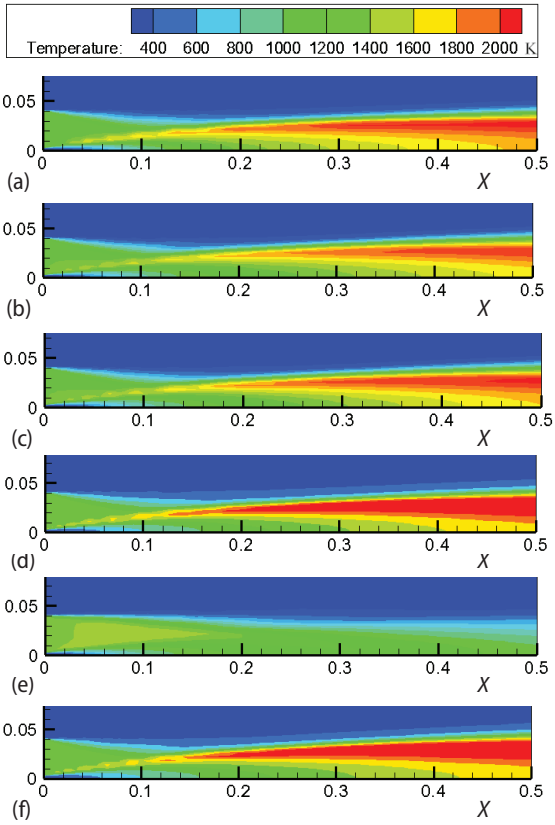

Figure 3. Temperature field (a) WD3, (b) 41-step, (c) KEE58, (d) DRM22, (e) GRI2.11, and (f) GRI3.0

The fig. 4 compares the temperature distribution in different chemical mechanism cases. The temperature distributions are similar at $x = 30$ mm, however show some differences at $x = 120$ mm. The hot co-flow entrained from the pilot zone will stabilize the flame to the burner, and this force leads extinction to occur. The flame will re-ignite at the downstream area when the mixing becomes less intense. When $x = 30$ mm, all the predicted result shows little difference. However, when $x = 120$ mm, there is a 200 K over-prediction at radial distance 15 mm $< z <$ 30 mm. The 41-step and KEE-58 mechanism match the measured temperatures quite well, albeit with some over-prediction at the peak values. Calculations of the DRM22 mechanism display a systematic over-prediction in peak temperature as well as a sharp drop-off in temperature on the rich side of both HM2 flames. Such an over-prediction of temperature was thought to stem from the turbulence-chemistry interaction model [20]. Similar temperature over-predictions have been noted previously for the DRM22 mechanism in comparison with the previous two mechanisms. Although, very satisfactory predictions were achieved with the modified k-ε turbulence model, the GRI2.11 mechanism is rather different from other mechanisms. When $x = 30$ mm, the result for GRI2.11 are in accordance with the prediction of Christo and Dally, but with an over-prediction of 200-300 K.

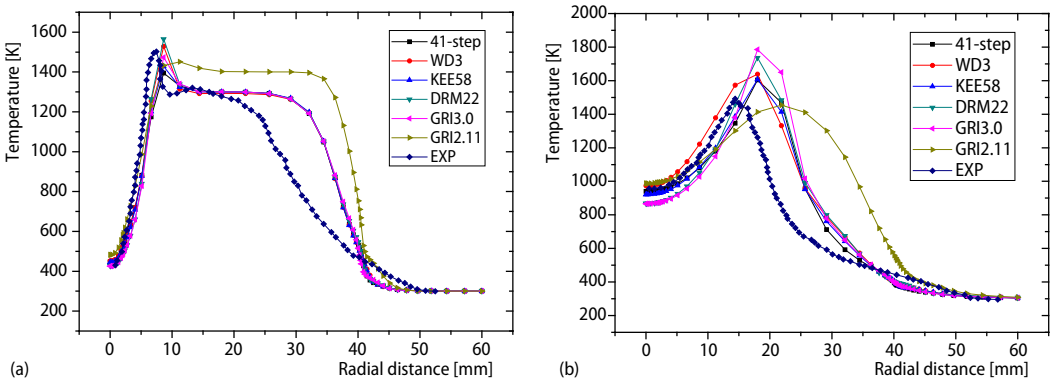

Figure 4. Temperature distribution at different axial distance (a) x = 30 mm, (b) x = 120 mm

In the fig. 5, the CO distributions of JHC flame at x = 30 mm and x = 120 mm are presented. From fig. 5(a), the content of CO reaches to its peak at z = 0-10 mm. Among all the mechanisms, the GRI3.0 mechanism shows the best agreement with the experiment result. The 41-step skeletal and DRM22 mechanisms over-predict the result. However, the KEE-58 mechanism under-predicts the concentration of CO. The global WD3 mechanism has the lowest accuracy. When x = 120 mm, the results show some discrepancies at z = 0-20 mm. Among all the reactions, the GRI3.0 mechanism has the highest precision. Other mechanisms may over-predict or under-predict the CO concentration.

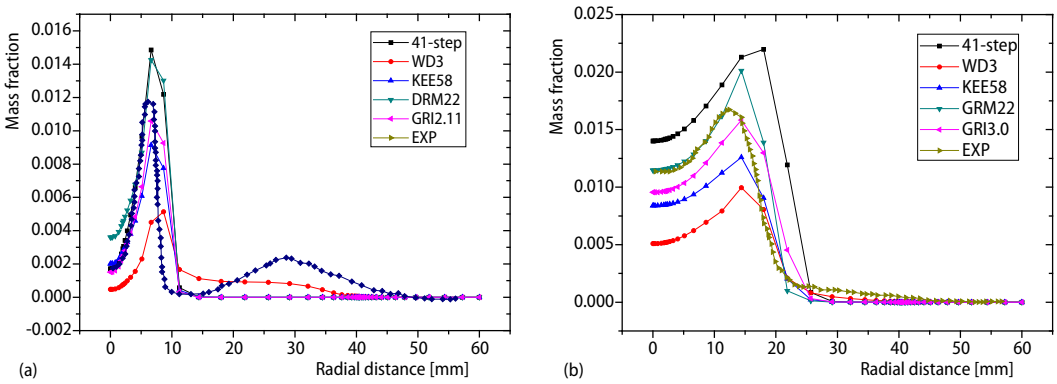

Figure 5. The CO mass fraction distribution at different axial distance (a) x = 30 mm (b) x = 120 mm

Figure 6 shows the mass fraction of OH at the flame region. The OH is generally considered as a flame marker which is one of the most important free radicals in high temperature combustion process. Controlling the reaction for the OH production is more sensitive to the temperature fluctuation at fuel/co-flow shear layer. From fig. 6(a), it can be easily found that all the mechanisms under-predict the OH content at x = 30 mm. However, when x = 120 mm, the predict result is higher than that of the experiment result.

The prediction for H_2O specie concentration is similar to the temperature distribution. Aside from GRI2.11 mechanism, all the other mechanism gives similar prediction results shown in fig. 7. The DRM22 mechanism reaches the highest, and then is the KEE-58 mecha-

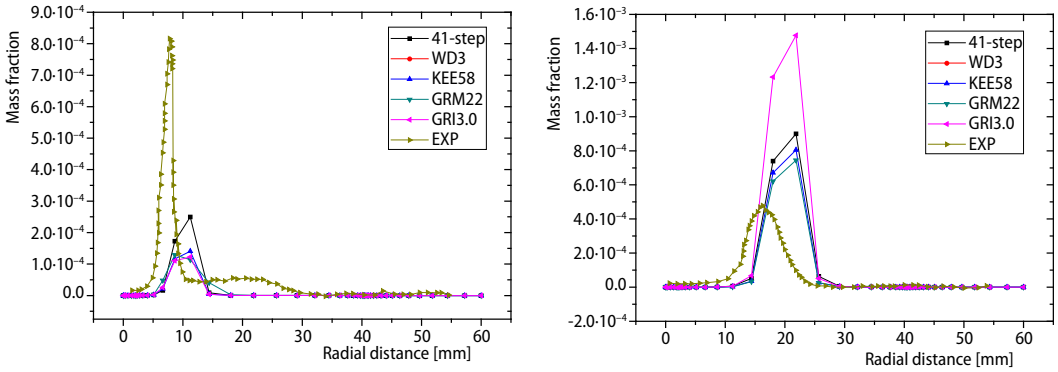

Figure 6. The OH mass fraction distribution at different axial distance (a) x = 30 mm (b) x = 120 mm

nism. The results of detailed mechanism, 41-step mechanism and WD3 mechanism are in co mmon with each other. When x = 120 mm, as shown in fig. 7(b), all the calculation results are similar with the experimental data. The KEE-58 mechanism and DRM22 mechanism give the best result, and GRI2.11 mechanism cannot provide a reasonable prediction results.

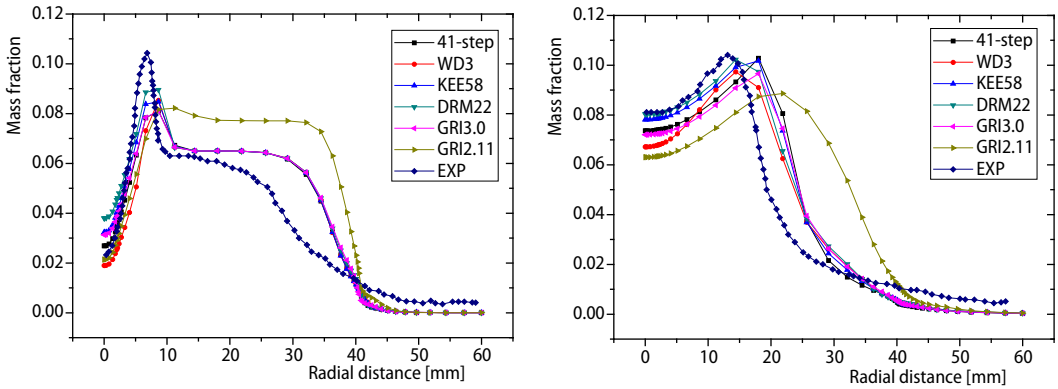

Figure 7. The H_2O mass fraction distribution at different axial distance (a) x = 30 mm (b) x = 120 mm

From the aforementioned experiment result, it can be found that the GRI3.0 mechanism shows the best prediction among all the six mechanisms. The DRM22 and 41-step skeletal mechanisms have similar result. The KEE-58 mechanism has a good temperature prediction, but under-predicts the most species content. The GRI2.11 has the similar result as the GRI3.0 mechanism at x = 30 mm, but it has a totally different temperature distribution at the downstream area. The global WD3 mechanism can give a reasonable temperature distribution but limited to some species distribution due to its simplicity.

Reaction analysis

Following the aforementioned discussion, we model the H_2/CH_4 combustion in a WSR model under the same conditions as these used in JHC burner. The experiment was carried out in a Chemkin code base. In the fig. 8, a scheme of WSR was shown. The V, P, τ denote the volume, pressure and residual time. The X_i^* and T_{in} are the inlet species and temperature. The X_{oi} and T_{out}

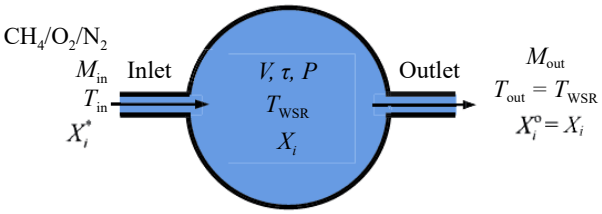

Figure 8. Scheme of WSR

represent the species fraction and temperature at the outlet. In the present paper, V and P are taken to be 67.4 cm^3 and 1.0 atm. The residence time τ and reactor temperature T_{WSR} can be set as 0.01 seconds and 1500 K. The equivalence ratio varies from 0.7 to 1.4. Fuel and the oxidant component are same as that in tab. 1.

In fig. 9, the reaction pathways of for CH_4/O_2 combustion at MILD environment are shown. Each arrow indicates the species conversion from its head to its tails. The mentioned conversion is addressed by elementary reactions in the GRI mechanism. The width and color indicate the relative importance of each reaction pathway. The global reaction pathways were influenced significantly by the temperature.

When $T_{WSR} > 1600$ K, the CH_4 reacts through route 1 in fig. 9(a): (CH_4-CH_3-CH_2O-HCO-CO-CO_2). The CH_4 was firstly attacked by OH and O radicals, losing H to form CH_3. CH_3 combines with OH and O to form CH_2O. Next, CH_2O was attacked by OH and H to form HCO radical. The HCO reacts with H_2O and O_2 to form CO. Finally, CO and OH transfer to CO_2. In the side reaction route, the CH_3 and OH react to form to methylene radical CH_2(s) and CH_2. CH_2(s) react with H_2O and N_2 to form CH_2, finally to CH_2O, HCO and CO. Some of CH_3 can transfer to CH_2OH directly with OH, then CH_2O, HCO and CO.

Importantly, when $T_{WSR} < 1600$ K, a new C_2 compound hydrogen reaction route is observed in fig. 9(b), two CH_3 radicals recombined to C_2H_6, then attacks OH to transfers to CO and H_2 through C_2H_x. The transfer route becomes (CH_4-CH_3-C_2H_6-C_2H_5-C_2H_4-C_2H_3-C_2H_2-CO) and (CH_4-CH_3-CH_2O-HCO-CO). The CH_3 cannot transfer to C_2H_x directly, but it can help them to dehydrogenate through a series of C_2H_x hydrocarbons.

The reaction route for GRI2.11 at $T_{WSR} > 1600$ K is shown in fig. 9(c). Compared with the reaction route in fig. 9(a), the main reaction route are similar with each other. However, when $T = 1700$ K, CH_3 reacts with OH to produce CH_3OH through R95 [OH+CH_3 (+M) = CH_3OH (+M)] and R147 [CH_2(s) +H_2O (+M) = CH_3OH (+M)]. CH_3OH will return to CH_4 through R162 (CH_3+CH_3OH = CH_3O+CH_4). The CH_4 oxidation pathway is disturbed by the intermediate electronic configurations CH_2(s) through R147. However for GRI3.0 mechanism, the CH_4 react through reaction R153 [CH_2(s) +CO_2 = CO+CH_2O] and R56 [H+CH_2O (+M) <=> CH_2OH (+M)]. Compared with the radical recombination, the reaction progress will consume a lot of energy in breaking the radical chain, which leads to a lower temperature region at the downstream area.

In fig. 9(d), the GRI2.11 oxidation process is similar with that of GRI3.0 mechanism. As expected, CH_4 can be partly recombined to the C_2 compound. The transfer route becomes (CH_4-CH_3-C_2H_6-C_2H_5-C_2H_4-C_2H_3-C_2H_2-CO) and (CH_4-CH_3-CH_2(s)-CO).

Conclusion

In the present paper, the performances of six different chemical mechanisms for CH_4/H_2 at MILD combustion condition were tested. These mechanisms include a global mechanism, three kinds of reduced mechanism, and two detailed mechanisms. They are WD3, 41-steps, KEE-58, DRM22, GRI2.11, and GRI3.0, respectively. The EDC model was applied in the experiment based on a FLUENT software. The temperature distribution and the specie distribu-

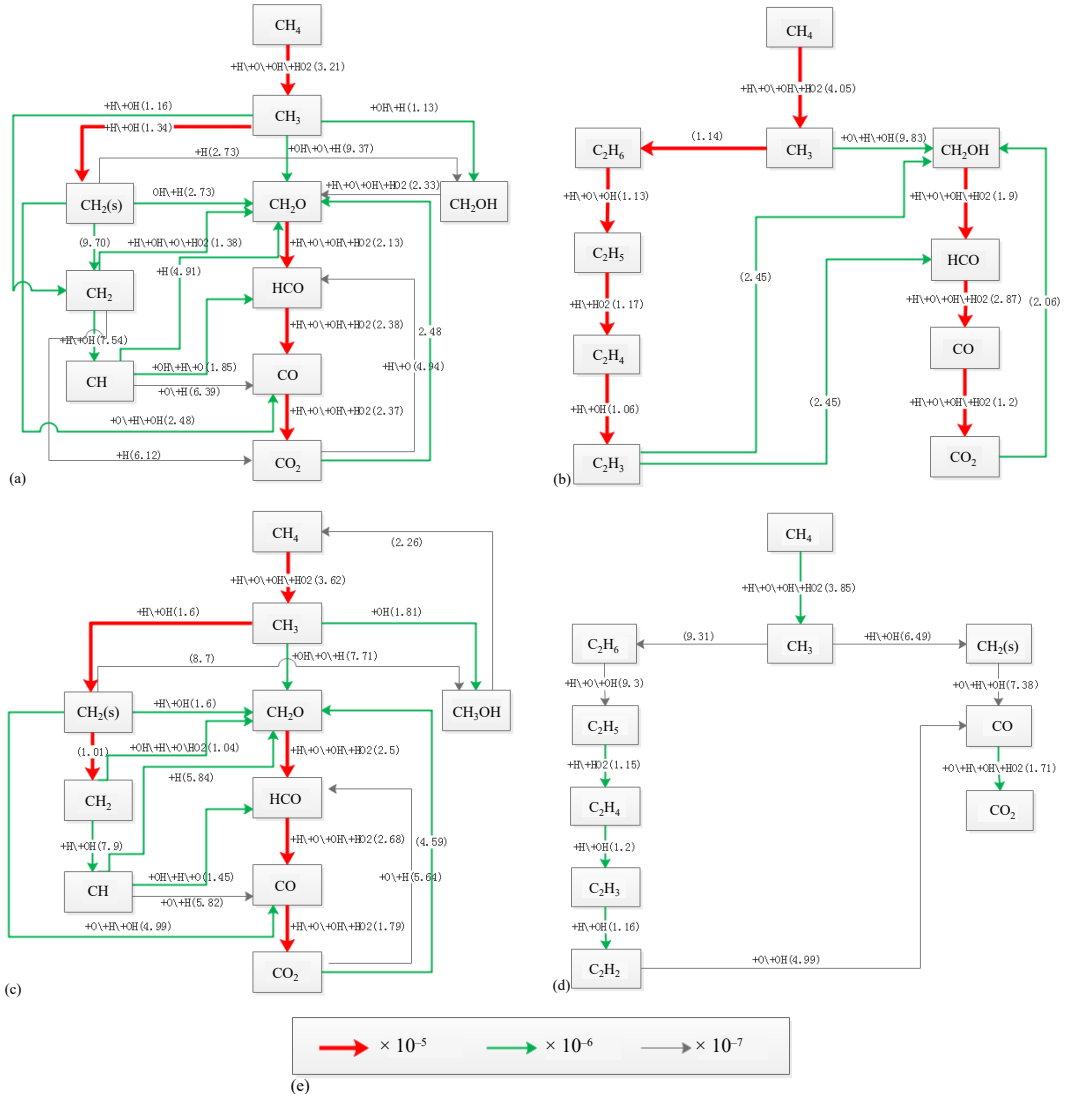

Figure 9. reaction route for GRI3.0 and GRI2.11 mechanisms; (a) GRI3.0 route1, (b) GRI3.0 route 2, (c) GRI2.11 route1, and (d) GRI2.11 route2

tions were investigated. Besides, the GRI2.11 and GRI3.0 were tested in a WSR model for reaction pathway. Several conclusions are evident at follows.

- The temperature distributions predicted by each chemical mechanisms were similar at $x = 30$ mm. The only difference is the peak values. The GRI3.0 mechanism gives the most precise peak values. The DRM22 and WD3 mechanisms give some over-prediction and the KEE-58 and 41-step mechanisms give some under-prediction. When $x = 120$ mm, all the predictions have an over-prediction of 200-300 K to the experiment data. When $x > 200$ mm, most flame will reignite at the downstream region. However, it distinguished for the GRI2.11 mechanism for the blowout character.

- For the main production H_2O and CO, most mechanisms give the similar prediction. The GRI3.0 mechanism gives the best result. The 41-step and DRM22 mechanisms predict a higher concentration and the KEE-58 mechanism predicts a lower concentration than the result. For the intermediate species OH, all the mechanism has significant error, they over-predict the results at x = 30 mm and under-predict the results at x = 120 mm.
- The two detailed mechanisms GRI3.0 and GRI2.11 were tested in a WSR reactor. The experiment result shows that under the same simulation conditions, the two mechanisms have some differences under MILD combustion conditions. Both the reactions have two pathways, Route 1: [CH_4-CH_3-CH_2O (CH_2OH)-HCO-CO-CO_2], and Route 2: [CH_4-CH_3--C_2H_x-(HCO)-CO-CO_2]. The R95 and R147 in GRI2.11 mechanism will consume a lot of energy in breaking the radical chain, which is responsible for the low temperature region at the downstream area.

Acknowledgment

The authors would like to express their thanks to the Institute of Turbomachinery, university of Xi'an Jiaotong University for the support financially.

References

[1] Cavaliere, A., de Joannon, M., Mild Combustion, *Progress in Energy and Combustion Science, 30* (2004), 4, pp. 329-366
[2] Dally, B. B., *et al.*, Structure of Turbulent Non-Premixed Jet Flames in a Diluted Hot Coflow, *Proceedings of the Combustion Institute, 29* (2002), 1, pp. 1147-1154
[3] Oldenhof, E., *et al.*, Role of Entrainment in the Stabilisation of Jet-In-Hot-Coflow Flames, *Combustion and Flame, 158* (2011), 8, pp. 1553-1563
[4] Wang, L., *et al.*, Comparison of Different Global Combustion Mechanisms under Hot and Diluted Oxidation Conditions, *Combustion Science and Technology, 184* (2012), 2, pp. 259-276
[5] Amir, M., *et al.*, Numerical Study of Flame Structure in the MILD combustion regime, *Thermal Science, 19* (2015), 1, pp. 21-34
[6] Parente, A., *et al.*, Investigation of the MILD Combustion Regime Via Principal Component Analysis, *Proceedings of the Combustion Institute, 33* (2009), 2, pp. 3333-3341
[7] Coelho, P., Peters, N., Numerical Simulation of a Mild Combustion Burner, *Combustion and Flame, 124* (2001), 3, pp. 503-518
[8] Christo, F. C., Dally, B. B., Modeling Turbulent Reacting Jets Issuing into a Hot and Diluted Coflow, *Combustion and Flame, 142* (2005), 1-2, pp. 117-129
[9] Kim, S. H., *et al.*, Conditional Moment Closure Modeling of Turbulent Nonpremixed Combustion in Diluted Hot Coflow, *Proceedings of the Combustion Institute, 30* (2005), 1, pp. 751-757
[10] Ihme, M., See, Y. C., LES Flamelet Modeling of a Three-Stream MILD Combustor: Analysis of Flame Sensitivity to Scalar Inflow Conditions, *Proceedings of the Combustion Institute, 33* (2011), 1, pp. 1309-1317
[11] Wang, F., *et al.*, Combustion of $CH_4/O_2/N_2$ in a Well Stirred Reactor, *Energy, 72* (2014), Aug., pp. 242-253
[12] Weber, R., On Emerging Furnace Design Methodology that Provides Substantial Energy Savings and Drastic Reductions in CO_2, CO and NO_x Emissions, *Journal of the Energy Institute, 72* (1999), 492, pp.77-83
[13] Dally, B. B., *et al.*, Structure of Turbulent Non-Premixed Jet Flames in a Diluted Hot Coflow, *Proceedings of the Combustion Institute, 29* (2002), 1, pp. 1147-1154
[14] Westbrook, C. K., Dryer, F. L., Simplified Reaction Mechanisms for the Oxidation of Hydrocarbon Fuels in Flames, *Combustion Science and Technology, 27* (2007), 1-2, pp. 31-43
[15] Yang, B., Pope, S. B., An Investigation of the Accuracy of Manifold Methods and Splitting Schemes in the Computational Implementation of Combustion Chemistry, *Combustion & Flame, 112* (1998), 1, pp. 16-32
[16] Bilger, R. W., *et al.*, On Reduced Mechanism for Methane-Air Combustion in Non-Premixed Flames, *Combustion and Flame, 80* (1990), 2, pp. 135-149

[17] Gran, I. R., Magnussen, B. F., A Numerical Study of a Bluff-Body Stabilized Diffusion Flame, Part 2, Influence of Combustion Modeling And Finite-Rate Chemistry, *Combustion Science and Technology, 119* (1996), 1-6, pp. 191-217
[18] Aminian, J., *et al.*, Key Modeling Issues in Prediction of Minor Species in Diluted-Preheated Combustion Conditions, *Applied Thermal Engineering, 31* (2011), 16, pp. 3287-3300
[19] Kim, Y. J., *et al.*, Prediction Performance of Chemical Mechanisms for Numerical Simulation of Methane Jet MILD Combustion, *Advances in Mechanical Engineering*, On-line first, https://doi.org/10.1155/2013/138729
[20] De, A., Dongre, A., Assessment of Turbulence-Chemistry Interaction Models in MILD Combustion Regime, Flow, *Turbulence and Combustion, 94* (2014), 2, pp. 439-478

Paper submitted: August 11, 2018
Paper revised: November 26, 2018
Paper accepted: December 7, 2018